

Selecting the Most Appropriate Model for Rheological Characterization of Synthetic Based Drilling Mud

Folayan J. Adewale^{1*}, Anawe P. Lucky², Abioye P. Oluwabunmi³ and Elehinafe F. Boluwaji⁴

¹⁻⁴ College of Engineering, Covenant University, Ota, Nigeria.

*Corresponding Author: folayanadewale03@yahoo.com.

1, 2 E-mail Ids: folayanadewale03@yahoo.com, adewale.folayan@covenantuniversity.edu.ng

*Orcid ID: 0000-0002-2479-2909

Abstract

Several mathematical models used in describing the rheology of non-Newtonian fluids includes but not limited to the following; The Power Law model, the Bingham Plastic Model, the Hershel-Buckley Model and the Casson Model. Selection of the best rheological model that accurately represent the shear stress-shear rate analysis is sine qua non to achieving correct results for pressure drops and hydraulic calculations.

Hence, in this study, in an effort to determining the best rheological model that accurately represent the rheology of Synthetic based Muds (SBMs), three different Synthetic based Fluids were used to form different Synthetic based Muds with the same composition throughout. These fluids are; Refined Bleached and Deodorized Coconut Oil (RBDCO), Methanol Trans esterified Palm Kernel Oil (TRANSPKO) and Inter Esterified Palm Kernel Oil (INTERPKO).

The rheological properties of these drilling muds were measured by using an automated 8-speed viscometer model 800. The dial readings of the viscometer were then converted to stresses by applying standard conversion factors and different non-Newtonian Models were used in computing the stress values.

In order to measure the degree of deviation of each model from the measured stress, two statistical methods were employed. These are; the Absolute Average Percentage Error (ϵ_{AAP}) and the Standard Deviation of Average Percentage Error ($SD\epsilon_{AAP}$). From the (ϵ_{AAP}) results, the Casson Rheological Model has the lowest (ϵ_{AAP}) for all the three mud samples while the Bingham Plastic Model showed a Marked deviation of it stresses from the measured stresses. The Trans esterified and Inter esterified PKOs also have the lowest standard deviation of percentage error with Casson model and the highest error was also seen in the Bingham plastic model. Hence, the Casson rheological model accurately predicts mud rheology and offers many advantages over the yield power law (Herschel-Buckley), the Bingham plastic and the power law rheological models because it more accurately characterizes mud behaviour across the entire shear rate conditions.

Keywords: Rheological models, Refined Bleached and Deodorized Coconut Oil (RBDCO), Methanol Trans esterified Palm Kernel Oil, Inter esterified Palm Kernel Oil, Absolute Average Percentage Error, Standard Deviation of average Percentage Error.

Nomenclatures

| | |
|------------------------|---|
| RBDCO | Refined Bleached and Deodorized Coconut Oil |
| TRANSPKO | Trans esterified Palm Kernel Oil |
| INTERPKO | Inter Esterified Palm Kernel Oil |
| (ϵ_{AAP}) | Absolute Average Percentage Error |
| ($SD\epsilon_{AAP}$) | Standard Deviation of Absolute Average Percentage Error |
| YP | Yield Point |
| PV | Plastic Viscosity |
| n | Flow Behaviour Index |
| k | Consistency Index |
| k_{oc} | Casson Plastic Viscosity |
| k_c | Casson Yield Stress |
| k_H | Herschel Buckley Consistency Index |
| n_H | Herschel Buckley Flow Index |
| τ_{oH} | Herschel Buckley Yield Stress |

Greek Symbols

| | |
|----------|--------------|
| μ | Viscosity |
| τ | Shear Stress |
| γ | Shear Rate |
| τ_o | Yield Stress |

Abbreviations

| | |
|------|------------------------------------|
| BPRM | Bingham Plastic Rheological Model |
| CRM | Casson Rheological Model |
| HBRM | Herschel-Buckley Rheological Model |
| PLRM | Power Law Rheological Model |

INTRODUCTION

Drilling fluids can be categorized into three main groups based on their composition and application. These are; Water based fluid (WBFs), Oil based fluids (OBFs) and Synthetic based fluids (SBFs). These fluids are used to perform some essential

functions which include but not limited to the following: control of abnormal formation pressure, suspension and release of drill cuttings and its removal from well, sealing of permeable formation to minimize formation damage and a host of other functions.

In nowadays oil well drilling operations, the synthetic based fluids (SBFs) have become the beautiful bride of the most Oil Companies because of its environmental friendliness, high biodegradability and lower toxicity [1]. Also, with SBFs, the rate of penetrations can be greatly maximized and thus reducing well drilling cost [2]

The ability of any drilling fluid to perform the afore mentioned functions is greatly vested on its rheology. Generally, fluids can be classified into, a Newtonian fluid whereby the shear stress is directly proportional to the shear rate and a single parameter known as viscosity characterizes the fluid and a non-Newtonian fluid whereby the shear stress is a function of prevailing shear rate.

Fluids behave differently with stress over time. While Rheopectic fluids increase in viscosity as stress increases such as gypsum pastes and printer inks, thixotropic fluids decrease in viscosity as stress increases overtime. Most Drilling fluids are non –Newtonian thixotropic shear thinning fluids with a yield stress in which viscosity is decreasing as shear rate increases [3]. Due to their compositions, drilling mud exhibit an internal structure which is liable to modification according to flowing and shear conditions [4]. This non-Newtonian flow behaviour has been attributed to mechanisms in which the shear stress, transmitted through the continuous medium, orients or distorts the suspended particles in opposition to the randomizing effects of Brownian motion [5].

In terms of both practical and fundamental significance, the two most important rheological properties of suspensions such as drilling muds are thixotropic and yield stress [6]. Hence, model that account for yield stresses are known as viscoplastic models or yield stress models [7].

The rheological model for non-Newtonian fluids may be grouped under three categories. We have the empirical model which are derived from examination of experimental data and an example is power law rheological model [8]. The structure model includes the casson model [9] and the Hershel Buckley model [10]. Also there is theoretical model which indicates factors that influences a rheological parameter and examples are, the Krieger-Dougherty model [5] for relative viscosity and the Bingham Plastic model [11].

The yield power law (Herschel-Buckley) rheological model accurately predicts mud rheology and offers many advantages over the Bingham plastic and power law rheological models because it more accurately characterizes mud behaviour across the entire shear rate [12]. Though the concept of yield stress in Hershel-Buckley model has been challenged because a fluid may deform minutely at stress values lower than the yield stress [13].

MATERIALS AND METHOD

Three synthetic base fluid samples were used to prepare synthetic based mud with the same mud component throughout as shown in Appendix A. These are: Refined, Bleached and Deodorized Coconut Oil (RBD CO), Trans-Esterified palm kernel oil (TRANSPKO) and Inter-Esterified Palm kernel oil (INTERPKO).

BASIC RHEOLOGICAL CONCEPTS

Rheology is the science of deformation and flow of matter. By making certain measurement on a fluid, it is possible to determine how that fluid will flow under a variety of conditions including temperature, pressure and shear rate.

The *viscosity of a fluid* (μ) is defined as the ratio of the shear stress (τ) to that of the shear rate (γ). Mathematically,

$$\mu = \frac{\tau}{\gamma} \quad (1)$$

The unit of viscosity can be expressed as Newton seconds/m² or Pascal seconds or poise (dyne.s/cm²).

Similarly, the *shear stress* (τ) is defined as the force required to sustain the movement of a particular type of fluid flowing through an area.

Mathematically,

$$\text{shear stress } (\tau) = \frac{\text{force}}{\text{area}} \quad (2)$$

The unit is N/m², Pascal or Dynes/cm².

Shear rate γ is defined as the rate of change of velocity when one layer of fluid passes over an adjacent layer divided by the distance between them. It is expressed in sec⁻¹ (reciprocal seconds). It can be converted to sec⁻¹ by using the equation:

$$\gamma = 1.703\gamma \quad (3)$$

Yield Point is a measure of the electrochemical or attractive force in a fluid. It is that part of resistance to flow that may be controlled by proper chemical treatment.

Mathematically, it is expressed as

$$YP = \theta_{300} - PV \quad (4)$$

The unit is lb. /100ft² or Pa.s

Where PV is the plastic viscosity in lb. /100ft²

Plastic Viscosity is described as that part of resistance to flow caused by mechanical friction. It is expressed as

$$PV = \theta_{600} - \theta_{300} \quad (5)$$

The unit is centipoise (cp)

RHEOLOGICAL MODEL OF DRILLING FLUIDS

Several mathematical model have been developed to describe the shear stress/ shear rate relationship of drilling fluids. These models are used to characterize flow properties in an effort to determine the ability of a fluid to perform specific functions [14]. There are two basic models for describing the rheology of drilling fluids viz: The Newtonian model where the shear stress (τ) is directly proportional to the shear rate ($\dot{\gamma}$) and the constant of proportionality is the fluid viscosity (μ) as shown in Fig. 1a and the non-Newtonian model where the fluid viscosity is not constant but a function of the shear stress and/or the prevailing shear rate or shear history as shown in Fig. 1b.

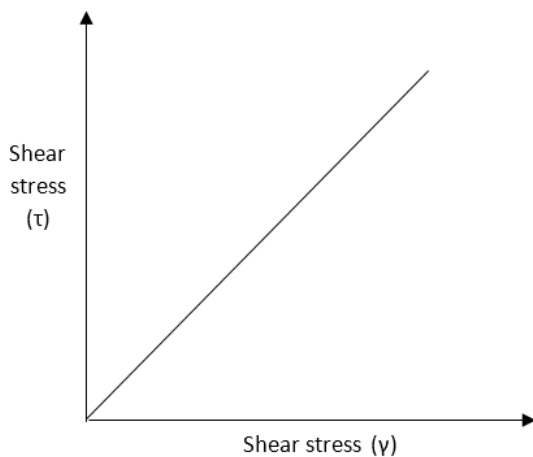


Figure 1a: Viscosity profile of Newtonian Fluid (Steffe, 1996)

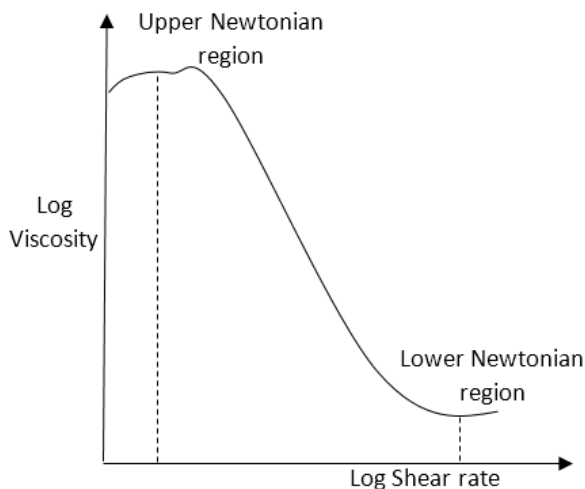


Figure 1b: Viscosity profile of non-Newtonian fluid

For Non- Newtonian model, there is usually a region at both low and high shear rate where the viscosity is independent or nearly independent of shear rate and a section in between that exhibits strong shear rate dependence [15].

The following mathematical models are used to describe the rheology of non-Newtonian fluids. These are:

1. Power Law model [8].
2. Bingham Plastic model [11].
3. Hershel Buckley Model [10].
4. Casson Model [9].

The power law model [8] is expressed as:

$$\tau = k\dot{\gamma}^n \quad (6)$$

Where n is the fluid flow behaviour index which indicates the tendency of a fluid to shear thin and it is dimensionless, and k is the consistency coefficient which serves as the viscosity index of the system and the unit is $\text{lb}/100\text{ft}^2\cdot\text{s}^n$ which can be converted to $\text{Pa}\cdot\text{s}^n$ by multiplying by a factor of 0.51 [16].

When $n < 1$, the fluid is shear thinning and when $n > 1$, the fluid is shear thickening. (Reiner, 1926).

The parameters k and n can be determined from a plot of $\log \tau$ versus $\log \dot{\gamma}$ and the resulting straight line's intercept is $\log k$ and the slope is n .

It can also be determined from the following equations.

$$n = 3.32 \log \left(\frac{\theta_{600}}{\theta_{300}} \right) \quad (7)$$

$$k = \frac{\tau}{\dot{\gamma}^n} = \frac{\theta_{600}}{1022^n} \quad (8)$$

But a linear regression or curve fitting of $\log \tau$ versus $\log \dot{\gamma}$ will provide statistically best values of k and n .

The k and n parameters can be gotten from taking the logarithmic function of Equation (6) as follows:

$$\log \tau = \log k + n \log \dot{\gamma} \quad (9)$$

And a plot of $\log \tau$ versus $\log \dot{\gamma}$ will result in a straight line with intercept $\log k$ and slope n as shown in Fig. 2 below:

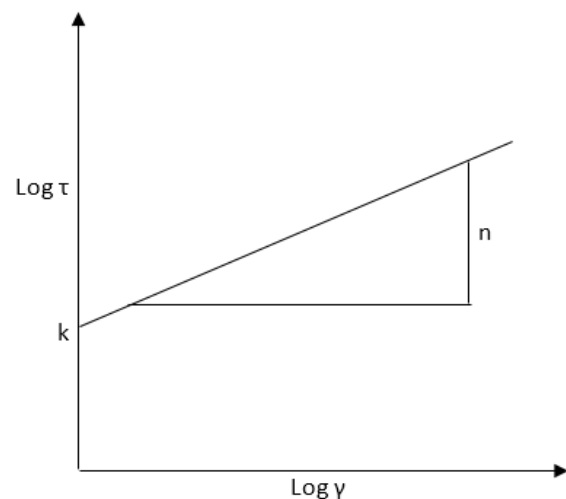


Figure 2: Power law logarithmic graphical Representation [8]

The power law model gives a better information in the low shear rate condition but has drawbacks in high shear rate conditions [17].

The Bingham plastic model is a two parameter model that is widely used in the drilling fluid industry to describe the flow characteristics of many type of muds. Mathematically, it can be represented as:

$$\tau = \tau_o + \mu_p \quad (10)$$

Where τ_o is the yield point and the unit is lb./100ft² or Pa.sⁿ and μ_p is the plastic viscosity and the unit is mPa.s (cp). The two parameters τ_o and μ_p can be determined from equations 4 and 5 respectively. Fluids that exhibit Bingham Plastic behaviour are characterized by a yield point (τ_o) and plastic viscosity (μ_p) that is independent of the shear rate.

However, it does not represent accurately the behaviour of the drilling fluid at very low shear rates (in the annulus) or at very high shear rate at the bit.

The Hershel- Bulkley Model is an extension of the Bingham Plastic model to include shear rate dependence. Mathematically, it is expressed as:

$$\tau = \tau_{oH} + k_H \gamma^{n_H} \quad (11)$$

Where γ is the shear rate (s⁻¹), τ is the shear stress (Pa), n_H is the flow behaviour index (dimensionless) and k_H is the HRBM consistency index in (Pa.sⁿ) and τ_{oH} is the HBRM yield stress (Pa).

If the yield stress of a fluid sample is known from an independent experiment, the parameters k_H and n_H can be determined by linearizing Equation (11) as follows:

$$\log(\tau - \tau_{oH}) = \log k + n \log (\gamma) \quad (12)$$

And a plot of $\log(\tau - \tau_{oH})$ versus $\log(\gamma)$ will result in a straight line with intercept $\log k_h$ and slope n_H respectively.

Fluids that exhibit a yield point and viscosity that is stress or strain dependent cannot be adequately described by the Bingham Plastic model. The Herschel Buckley model corrects this deficiency by replacing the plastic viscosity term in the Bingham Plastic model with a power law expression. However, the concept of yield stress has been challenged [13] because a fluid may deform minutely at stress values lower than the yield stress.

The Yield stress is normally taken as the 3 rpm reading.

The Casson Rheological Model is a structure based model (Casson, 1959) used to describe the flow of visco-elastic fluids. This model has a more gradual transition from Newtonian to the Yield region. Mathematically, the Casson model is expressed as

$$\tau^{\frac{1}{2}} = k_{oc}^{\frac{1}{2}} + k_c^{\frac{1}{2}} \gamma^{\frac{1}{2}} \quad (13)$$

Where k_{oc} is Casson yield stress (Pa.s), k_c is Casson plastic viscosity in mPa.s

The parameters k_{oc} and k_c can be obtained from the straight line that is drawn when the square root of shear stress ($\tau^{0.5}$) is plotted against the square root of shear rate ($\gamma^{0.5}$) with the slope k_c and intercept k_{oc} .

The Casson yield stress is calculated as the square of the intercept, $\tau_{oc} = (k_{oc})^2$ and the Casson plastic viscosity is the square of the slope $\eta_{ca} = (k_c)^2$.

RESULTS AND DISCUSSION.

Analysis of the RBDCO Mud Sample

Table 1: Viscometer Readings for RBDCO.

| Speed (RPM) | Dial Reading(lb/100ft ²) | Shear rate (s ⁻¹) |
|-------------|--------------------------------------|-------------------------------|
| 600 | 70 | 1022 |
| 300 | 40 | 511 |
| 200 | 34 | 340.60 |
| 100 | 19 | 170.30 |
| 60 | 12 | 102.18 |
| 30 | 8 | 51.09 |
| 6 | 6 | 10.22 |
| 3 | 4 | 5.11 |

Determination of Model Parameters for the Rheological Model of RBDCO

The power law rheological model parameters (n and k) were obtained by regression analysis by using Equation (6). Based on this equation, a plot of $\log \tau$ versus $\log \gamma$ as shown in Fig. 3 gives a straight line with Equation (14).

$$\log \tau = 0.5241 \log \gamma + 0.1597 \quad (14)$$

Hence, the power law equation for RBDCO can be expressed as;

$$\tau = 0.7364 \gamma^{0.5241} \quad (15)$$

Eq. (15) is used to generate the power law stress values shown in table 2.

The yield stress (τ_o) for Bingham plastic model is obtained by using equation 4 as 10 lb/100ft² which can be converted to Pascal by multiplying by 0.51 and the plastic viscosity is obtained by using Equation (5) as 0.0153 mPa.s. Hence, the Bingham plastic stresses for RBDCO can be expressed as

$$\tau_o = 5.10 + 0.0153 \gamma \quad (16)$$

Eq. (16) is used to generate the Bingham plastic stresses as shown in Table 2.

The Hershel-Buckley yield stress τ_{oH} is taken as the Θ_3 yield stress to be 2.04 Pa and the flow behaviour index and consistency index were obtained by regression analysis using

Equation (12), based on this equation, a plot of $\log(\tau - \tau_{oH})$ against $\log \gamma$ as shown in Fig. 4 gives a straight line as shown in Equation (17)

$$\log(\tau - \tau_{oH}) = 0.7985 \log \gamma - 0.6174 \quad (17)$$

Hence the Hershel Bulkley equation for RBDCO is given as

$$\tau = 2.04 + 0.1231(\gamma^{0.7985}) \quad (18)$$

Eq. (18) is used to generate the Hershel-Buckley stresses shown in table 2.

The Casson yield stress (k_{oc}) and the Casson plastic viscosity (k_c) are obtained by a plot of $\tau^{0.5}$ versus $\gamma^{0.5}$ as shown in Fig. 5. Based on this plot, the Casson equation for RBDCO is given as

$$\tau^{0.5} = 2.311^{0.5} + 0.0465^{0.5}(\gamma^{0.5}) \quad (19)$$

This can be converted to pascal by multiplying by 0.51 to give Equation (20)

$$\tau^{0.5} = 1.17861^{0.5} + 0.02372^{0.5}(\gamma^{0.5}) \quad (20)$$

Eq. (20) is used to generate the Casson stresses shown in table 2.

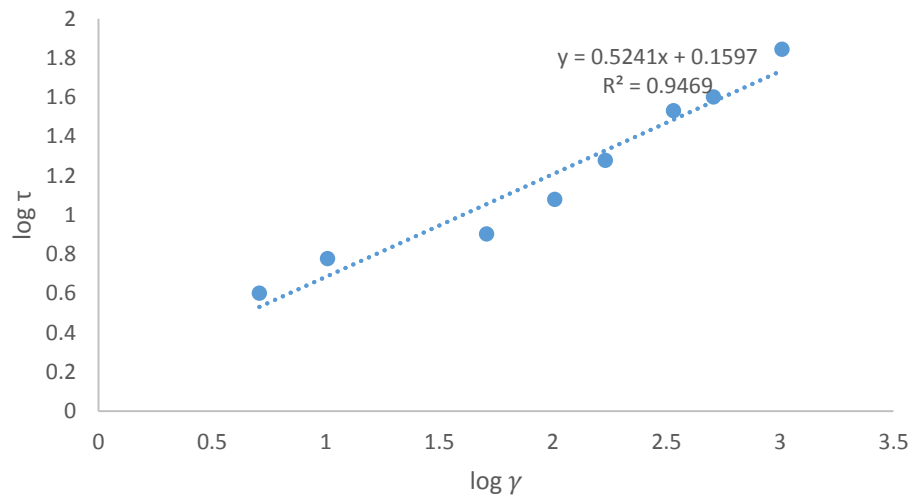


Figure 3: Power law Rheogram for RBDCO

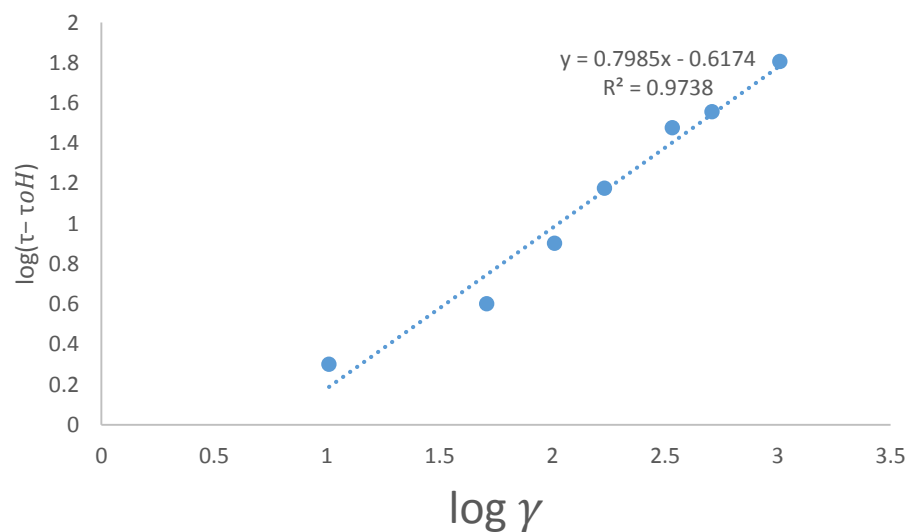


Figure 4: Hershel-Buckley Rheogram for RBDCO

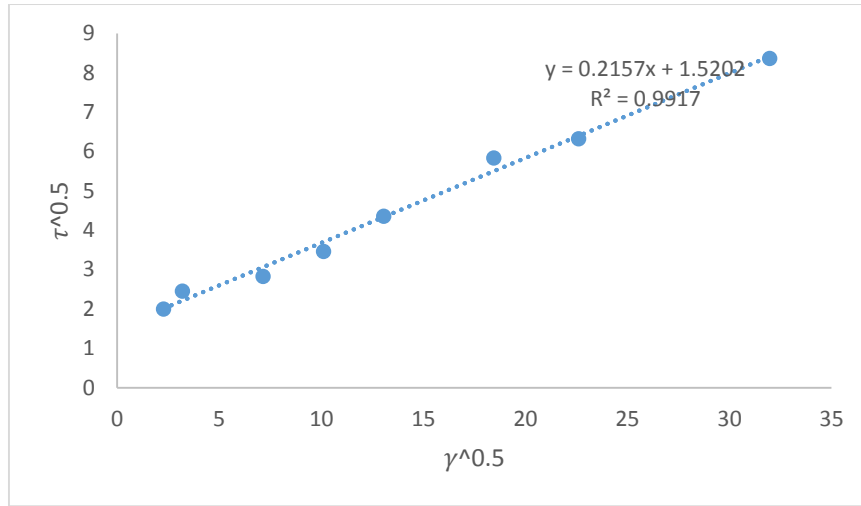


Figure 5: Casson Rheogram for RBDCO

Table 2.: Stress Values of Different Models for RBDCO Mud.

| Speed (RPM) | Dial (lb/100ft ²) | shear rate(S ⁻¹) | Measured (Pa) | PLRM (Pa) | BPRM (Pa) | HBRM (Pa) | CRM (Pa) |
|-------------|-------------------------------|------------------------------|---------------|-----------|-----------|-----------|----------|
| 600 | 70 | 1022 | 35.7 | 27.8574 | 20.7366 | 33.1696 | 36.1216 |
| 300 | 40 | 511 | 20.4 | 19.3352 | 12.9183 | 19.9378 | 20.8646 |
| 200 | 34 | 340.6 | 17.34 | 15.6326 | 10.3112 | 14.9856 | 15.4332 |
| 100 | 19 | 170.3 | 9.69 | 10.8716 | 7.7056 | 9.4831 | 9.5843 |
| 60 | 12 | 102.18 | 6.12 | 8.3185 | 6.6634 | 6.99 | 6.9841 |
| 30 | 8 | 51.09 | 4.08 | 5.785 | 5.8817 | 4.886 | 4.7816 |
| 6 | 6 | 10.22 | 3.06 | 2.4891 | 5.2563 | 2.8272 | 2.4902 |
| 3 | 4 | 5.11 | 2.04 | 1.7314 | 5.1782 | 2.4926 | 2.0558 |

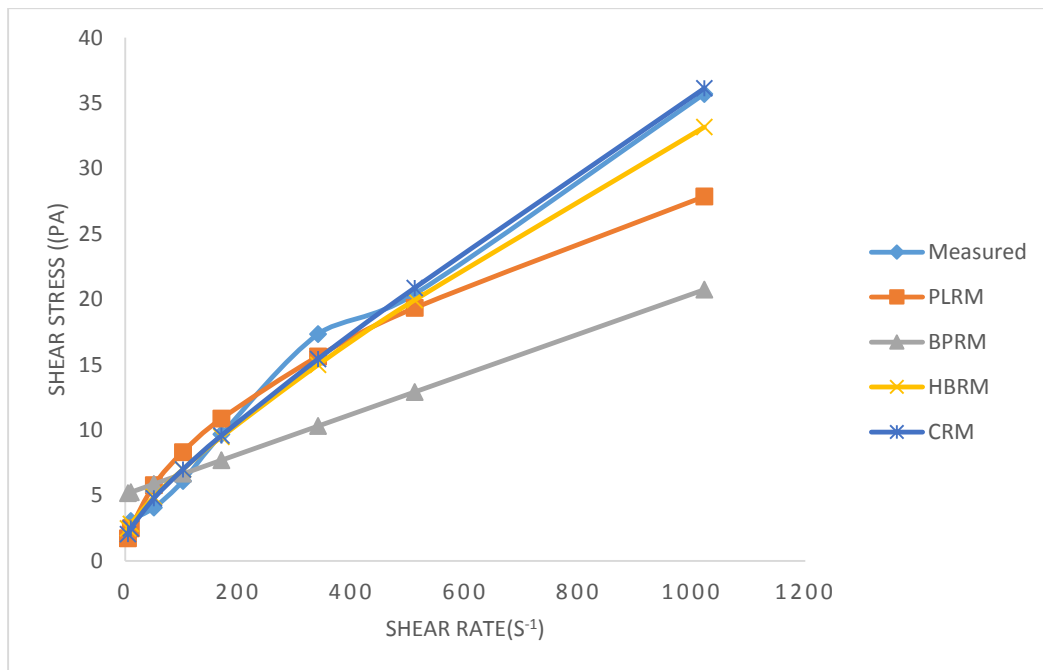


Figure 7: Shear Stress-Shear Rate Graph of Different Models for RBDCO

Analysis of TRANS PKO MUD SAMPLE.

Table 3: Viscometer Readings for TRANSPKO Mud

| Speed (RPM) | Dial Reading(lb/100ft ²) | Shear rate (s ⁻¹) |
|-------------|--------------------------------------|-------------------------------|
| 600 | 79 | 1022 |
| 300 | 45 | 511 |
| 200 | 41 | 340.06 |
| 100 | 25 | 170.30 |
| 60 | 14 | 102.18 |
| 30 | 11 | 51.09 |
| 6 | 8 | 10.22 |
| 3 | 6 | 5.11 |

Determination of Model Parameters for TRANSPKO

The n and k parameters for power law were obtained by a plot of log τ versus log γ as shown in Fig.7 to give a straight line with the Equation (21).

$$\log \tau = 0.4757 \log \gamma + 0.3573 \quad (21)$$

Hence the PLRM for **TRANSPKO** is given as:

$$\tau = 1.1611\gamma^{0.4757} \quad (22)$$

Eq. (22) is used to generate the power law stresses in Table 4.

The plastic viscosity is obtained by using Equation (5) as 0.01734 mPa.s while the yield stress is 5.61 Pa. Hence, the Bingham Plastic equation for **TRANSPKO** is:

$$\tau_o = 5.61 + 0.01734\gamma \quad (23)$$

Eq. (23) is used to generate the power law stresses in Table 4.

Similarly, the resulting straight line equation from the plot of log ($\tau - \tau_{oH}$) against log γ for Hershel-Bulkley equation for **TRANSPKO** as shown in Fig.8 is

$$\log(\tau - \tau_{oH}) = 0.8175 \log \gamma - 0.6075 \quad (24)$$

Hence the Hershel Buckley equation for **TRANSPKO** is given as:

$$\tau = 3.06 + 0.1259(\gamma^{0.8175}) \quad (25)$$

Eq. (25) is used to generate the HBRM stresses in Table 4

Also, the equation of straight line obtained from the plot of $\tau^{0.5}$ versus $\gamma^{0.5}$ for Casson in lb. /100ft² as shown in Fig. 9 is:

$$\tau^{0.5} = 3.7694^{0.5} + 0.0479^{0.5}(\gamma^{0.5}) \quad (26)$$

Converting to Pa, gives,

$$\tau^{0.5} = 1.9224^{0.5} + 0.02443^{0.5}(\gamma^{0.5}) \quad (27)$$

Eq. (27) is used to generate the Casson stresses in Table 4

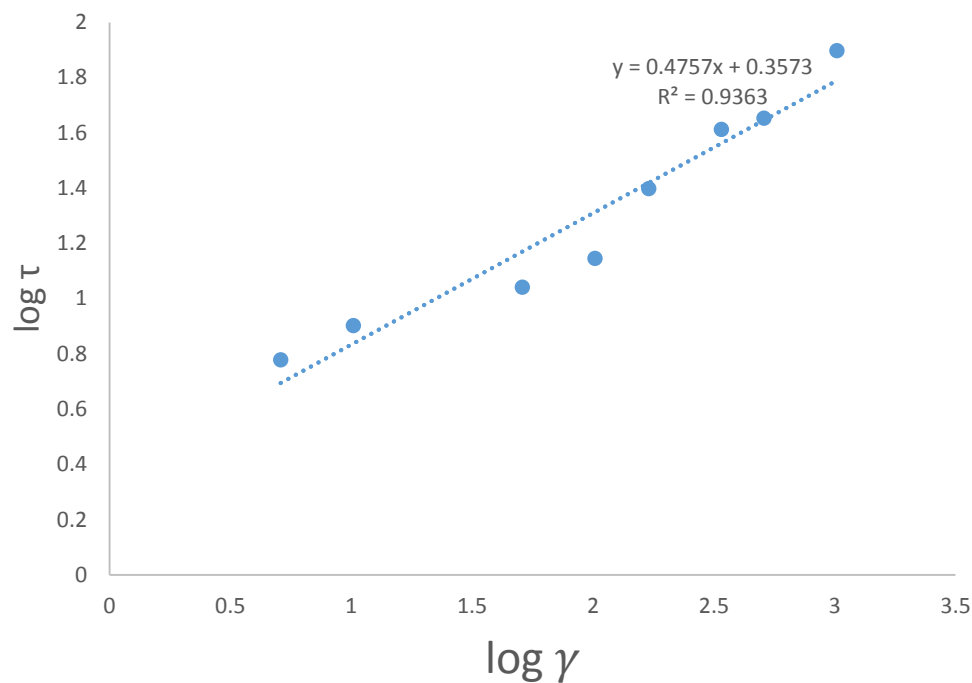


Figure 7: Power Law Rheogram for TRANSPKO

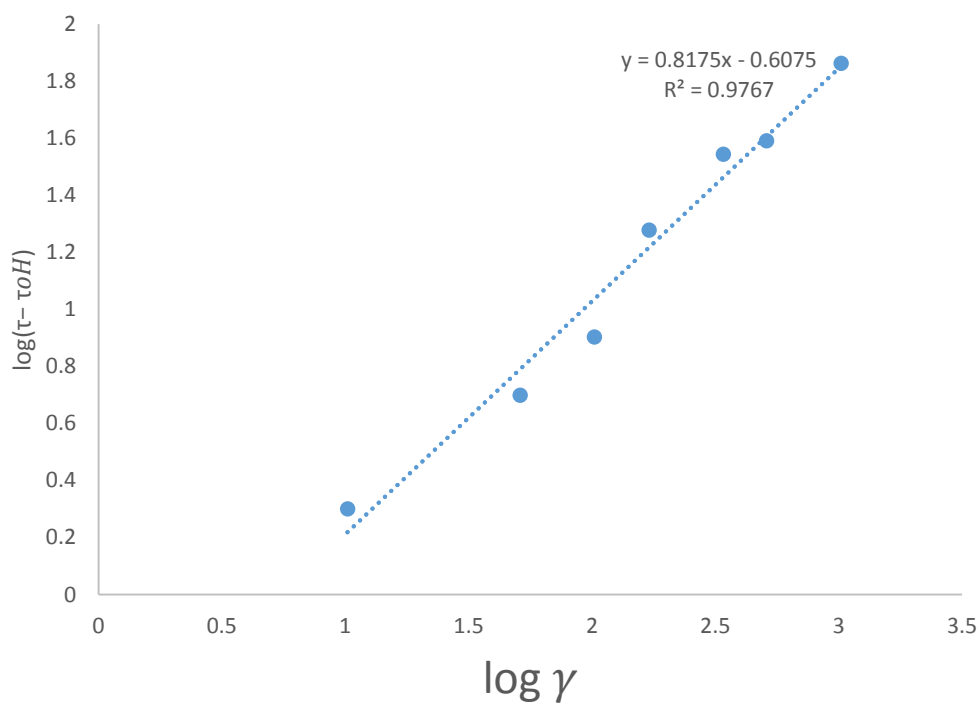


Figure 8: Hershel-Buckley Rheogram for TRANSPKO

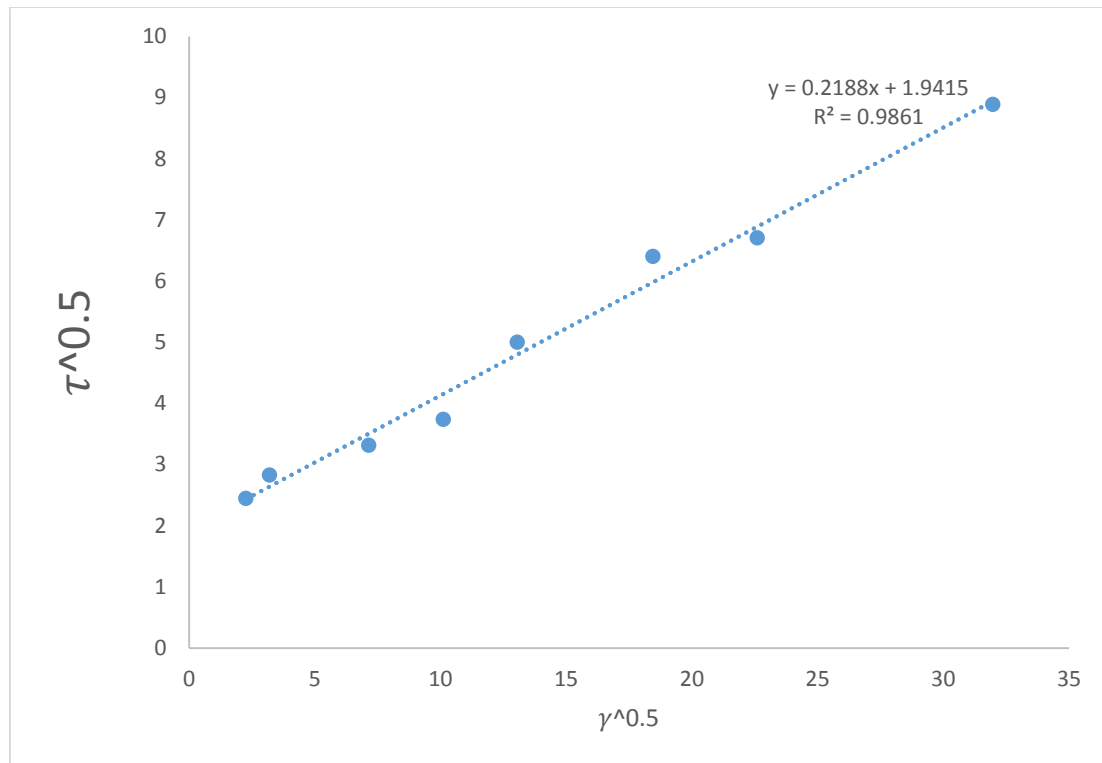


Figure 9: Casson Rheogram for TRANSPKO

Table 4: Stress Values of Different Models for TRANS PKO Mud

| Dial speed RPM | Dia Readings (lb/100ft ²) | Shear rate (S ⁻¹) | Measured (Pa) | PLRM (Pa) | BPRM (Pa) | HBRM (Pa) | CRM (Pa) |
|-------------------|---|----------------------------------|------------------|--------------|--------------|--------------|-------------|
| 600 | 79 | 1022 | 40.29 | 31.3655 | 23.3315 | 39.3943 | 40.7269 |
| 300 | 45 | 511 | 22.95 | 22.5534 | 14.4707 | 23.6769 | 24.1935 |
| 200 | 41 | 340.6 | 20.91 | 18.5971 | 11.516 | 17.8579 | 18.235 |
| 100 | 25 | 170.3 | 12.75 | 13.3735 | 8.563 | 11.4567 | 11.7348 |
| 60 | 14 | 102.18 | 7.14 | 10.4885 | 7.3818 | 8.5903 | 8.7971 |
| 30 | 11 | 51.09 | 5.61 | 7.5424 | 6.4959 | 6.198 | 6.2669 |
| 6 | 8 | 10.22 | 4.08 | 3.5076 | 5.7872 | 3.9019 | 3.557 |
| 3 | 6 | 5.11 | 3.06 | 2.5224 | 5.6986 | 3.5377 | 3.0265 |

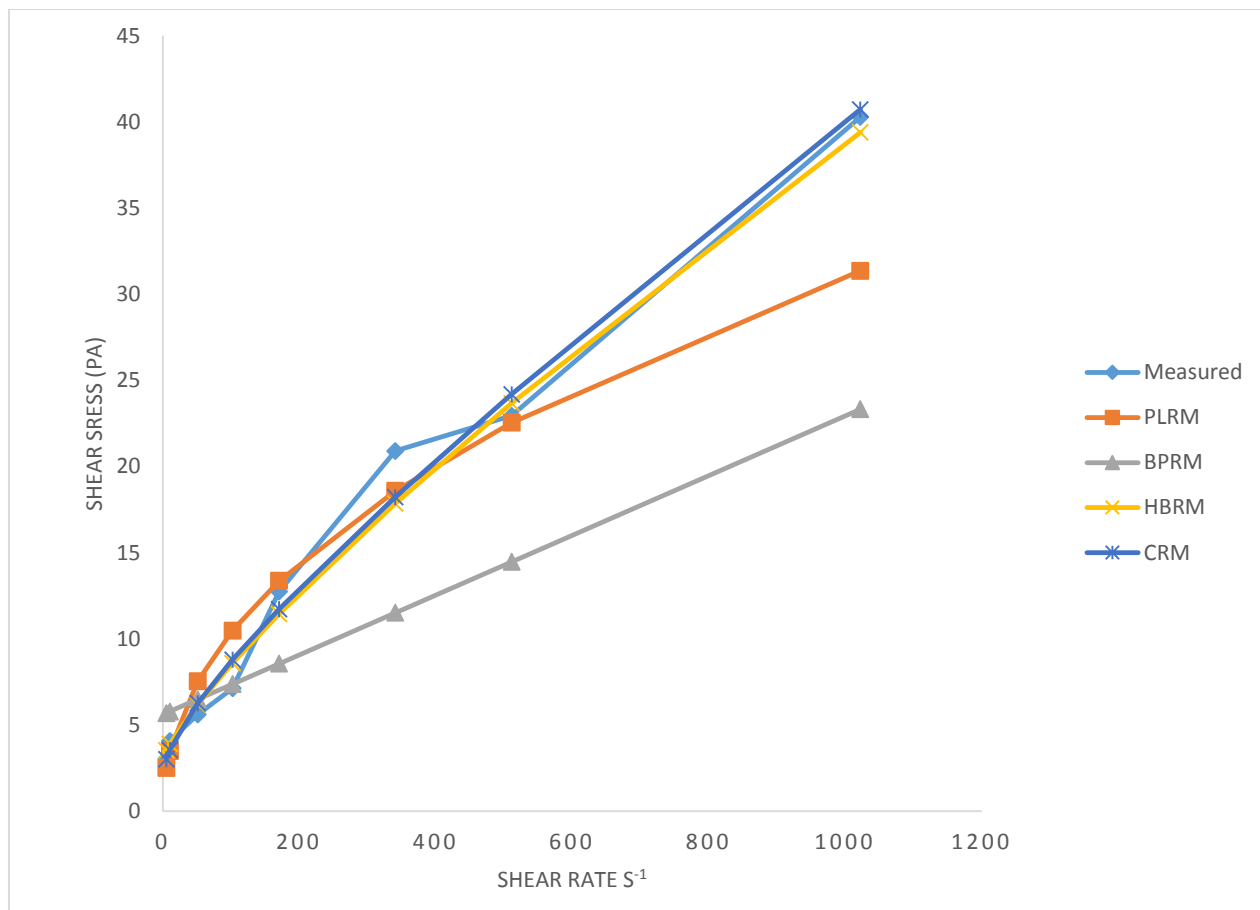


Figure 10: Shear Stress-Shear Rate Graph of Different Models for TRANSPKO

ANALYSIS OF INTER PKO Mud Sample.

Table 5: Viscometer Readings for INTERPKO Mud.

| Speed (RPM) | Dial Readings (lb/100ft ²) | Shear rate (s ⁻¹) |
|-------------|--|-------------------------------|
| 600 | 57 | 1022 |
| 300 | 34 | 511 |
| 200 | 26 | 340.60 |
| 100 | 21 | 170.30 |
| 60 | 17 | 102.18 |
| 30 | 11 | 51.09 |
| 6 | 8 | 10.22 |
| 3 | 6 | 5.11 |

Determination of Model Parameters for INTERPKO Mud Sample.

Using the same method for RBDCO and TRANSPKO, a plot of $\log \tau$ versus $\log \gamma$ as shown in Fig. 11 gives a straight line with Equation (28).

$$\log \tau = 0.3981 \log \gamma + 0.4551 \quad (28)$$

Hence the PLRM for inter esterified PKO is given as

$$\tau = 1.4544\gamma^{0.3981} \quad (29)$$

Eq. (29) is used to generate the power law stresses in Table 6.

The plastic viscosity is obtained by using Equation (5) as 0.01173 mPa.s while the yield stress is 5.61 Pa from Equation (4). Hence, the Bingham plastic rheology model for inter-esterified PKO is given as

$$\tau_o = 5.61 + 0.01173\gamma \quad (30)$$

Eq. (30) is used to generate the power law stresses in Table 6.

A plot of $\log (\tau - \tau_{oH})$ against $\log \gamma$ as shown in Fig.12 gives a straight line with Equation (31)

$$\log (\tau - \tau_{oH}) = 0.6984 \log \gamma - 0.4211 \quad (31)$$

Hence the HRBM for inter-esterified PKO is

$$\tau = 3.06 + 0.1934(\gamma^{0.6984}) \quad (32)$$

Eq. (32) is used to generate the power law stresses in Table 6.

The equation of straight line obtained from the plot of $\tau^{0.5}$ versus $\gamma^{0.5}$ for Casson in lb. /100ft² as shown in Fig.13 is:

$$\tau^{0.5} = 5.0073\gamma^{0.5} + 0.02700\gamma^{0.5} \quad (33)$$

Converting to Pa gives:

$$\tau^{0.5} = 2.5537\gamma^{0.5} + 0.01377\gamma^{0.5} \quad (34)$$

Eq.(34) is used to generate the Casson law stresses in Table 6

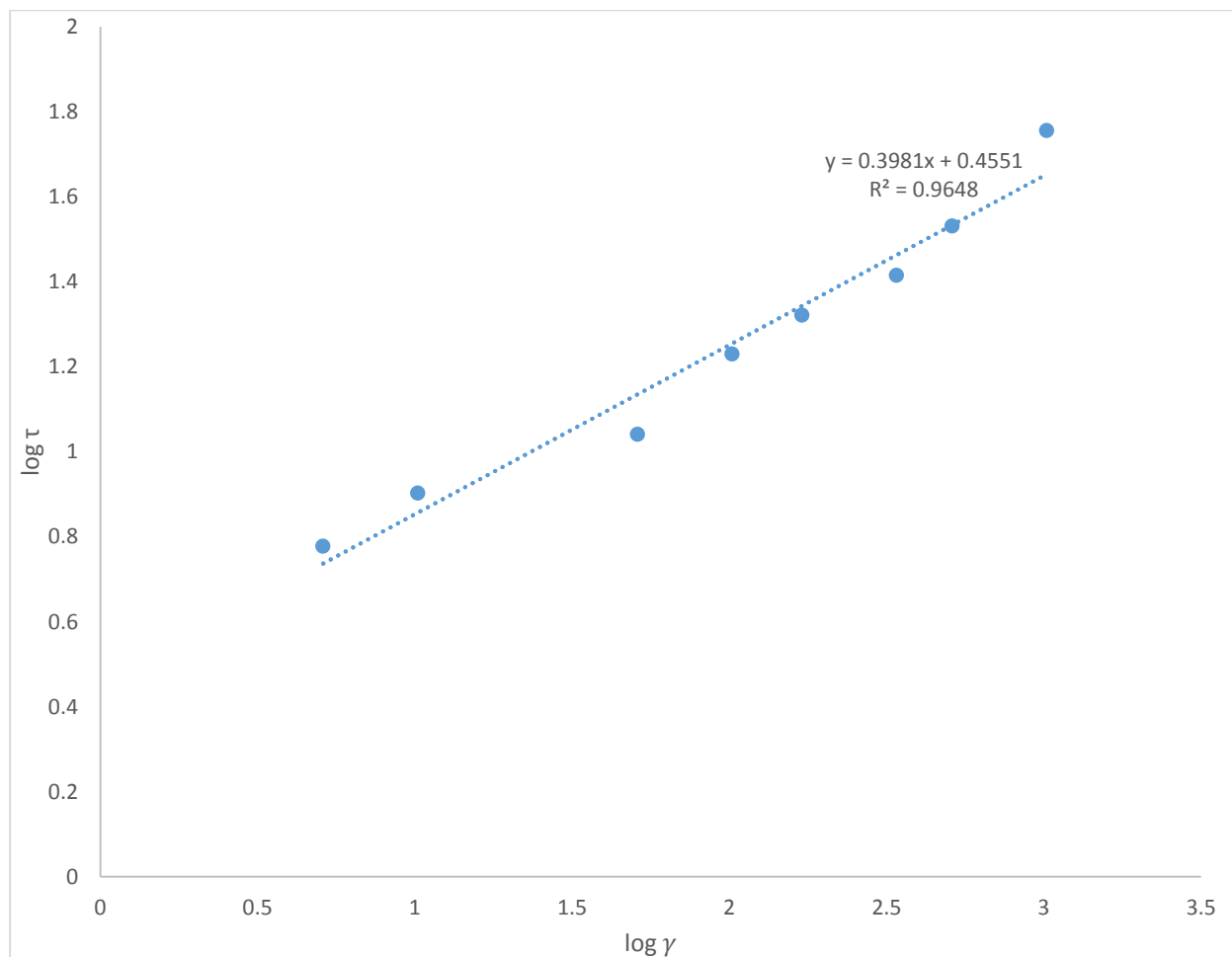


Figure 11: Power Law Rheogram for INTERPKO

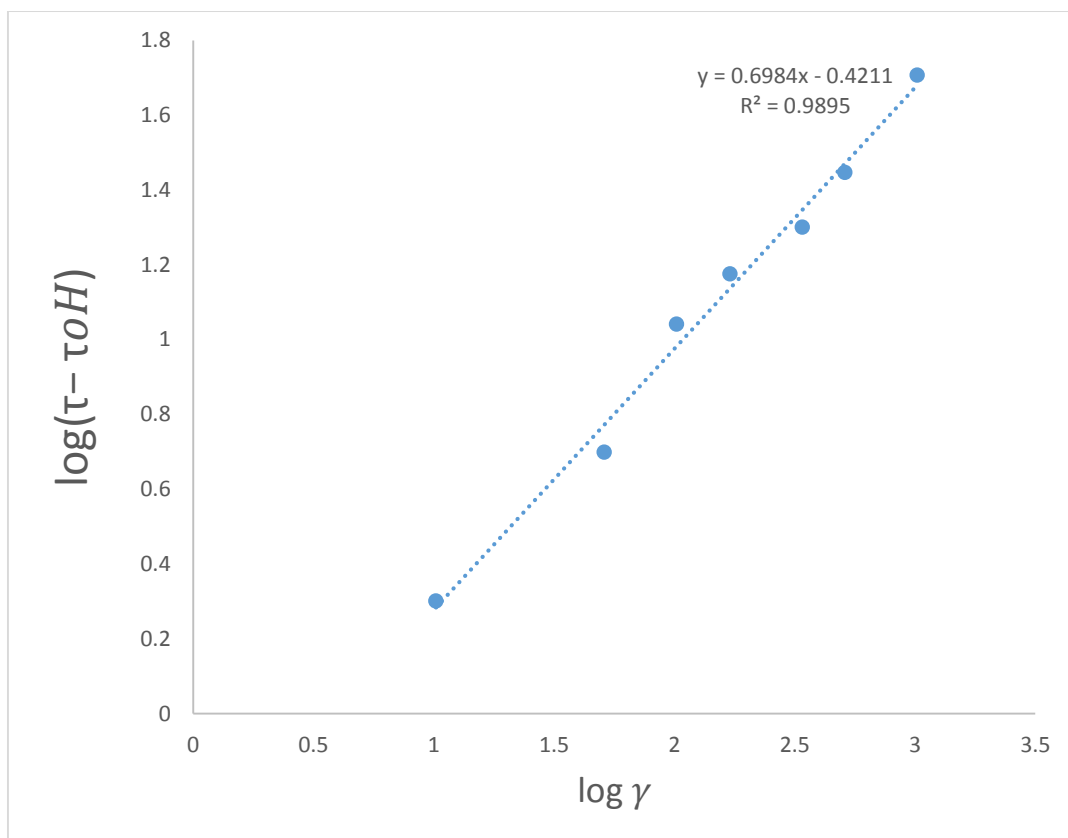


Figure 12: Hershel-Buckle Rheogram for INTERPKO Mud Sample

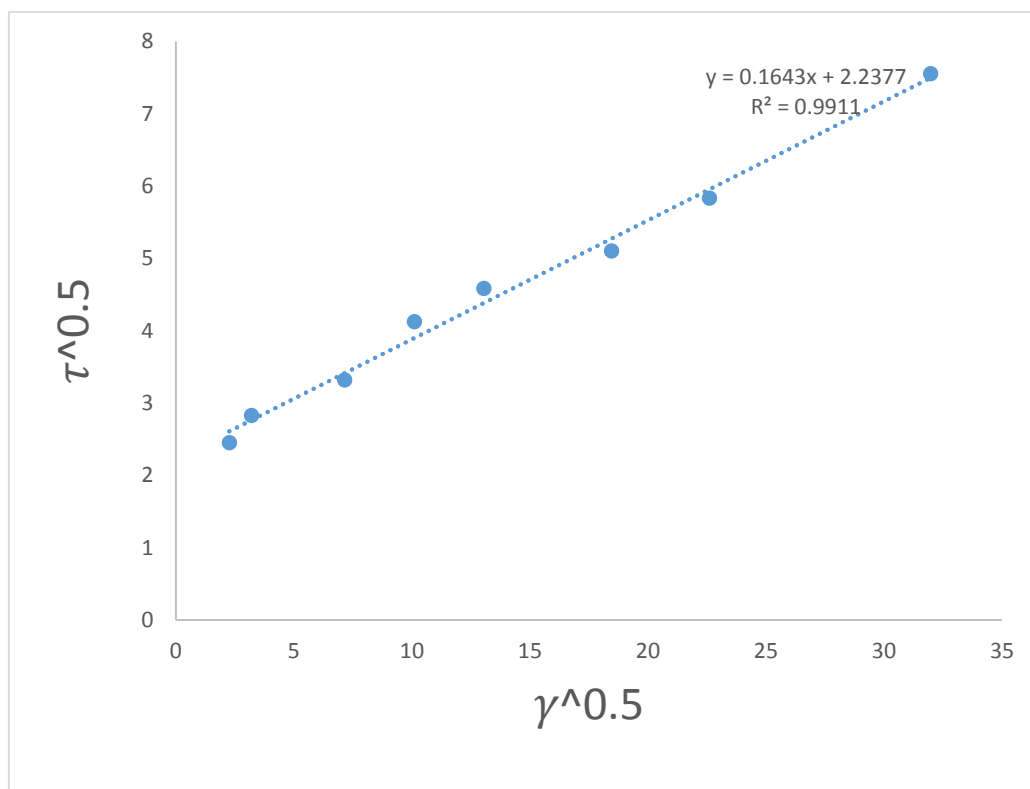


Figure 13: Casson Rheogram for INTER PKO Mud Sample

Table 6: Stress Values of Different Models for INTER PKO Mud Sample.

| Dial speed (RPM) | Dial (lb/100ft) | Shear rate (S ⁻¹) | Measured(Pa) | PLRM (Pa) | BPRM (Pa) | HBRM (Pa) | CRM (Pa) |
|---------------------|-----------------|----------------------------------|--------------|--------------|--------------|--------------|-------------|
| 600 | 57 | 1022 | 29.07 | 22.9476 | 17.5981 | 27.5078 | 28.6123 |
| 300 | 34 | 511 | 17.34 | 17.4126 | 11.604 | 18.1261 | 18.0659 |
| 200 | 26 | 340.6 | 13.26 | 14.817 | 9.6052 | 14.409 | 14.1637 |
| 100 | 21 | 170.3 | 10.71 | 11.244 | 7.6076 | 10.0539 | 9.7921 |
| 60 | 17 | 102.18 | 8.67 | 9.1749 | 6.8086 | 7.9553 | 7.7512 |
| 30 | 11 | 51.09 | 5.61 | 6.9625 | 6.2093 | 6.0768 | 5.9375 |
| 6 | 8 | 10.22 | 4.08 | 3.6686 | 5.7298 | 4.0403 | 3.8931 |
| 3 | 6 | 5.109 | 3.06 | 2.784 | 5.6699 | 3.6641 | 3.4717 |

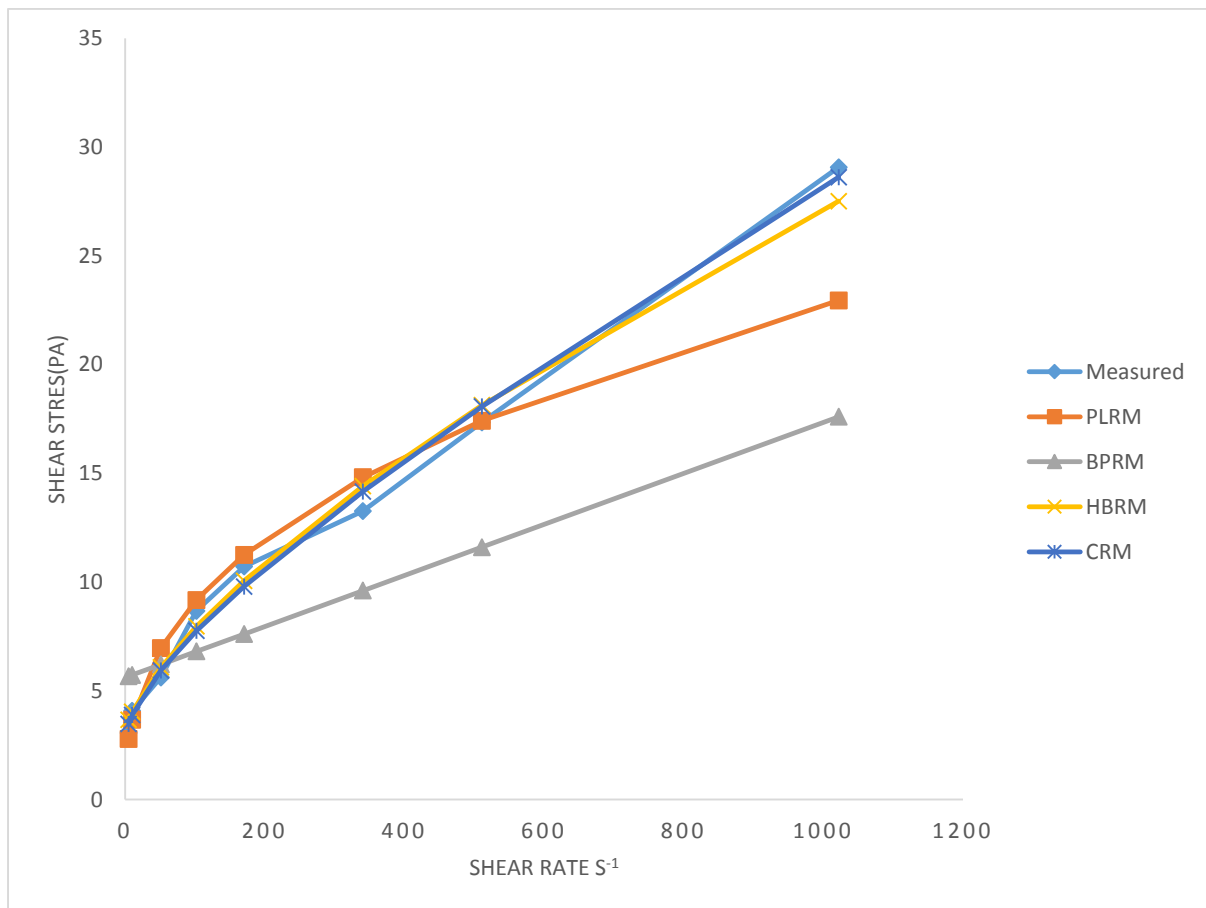


Figure 14: Shear Stress-Shear Rate Graph of Different Models for INTERPKO

DISCUSSION

From Figures 6,10 and 14 for stress values predicted by different rheological models for RBDKO, TRANSPKO and INTERPKO respectively, it can be inferred that the stress values predicted by the Bingham Plastic rheological model are

lower at high shear rate conditions compared to the measured stress values but higher at lower shear rate conditions. The higher stress values at lower shear rate conditions is attributed to the fact that the Bingham Plastic model includes a yield point that is positive shear stress at zero shear rate [18].

Also, the stress values of Power law rheological model are lesser than the measured values at the onset of high and low shear rate conditions. This can be attributed to the partial rebuilding of the fluid microstructure previously broken down by pre-shear [19]. Hence, the results of the Power law rheological model agree with Lauzon and Reid [17] because it cannot represent accurately the behaviour of the drilling fluid at very low shear rate in the annulus or a very high shear rate at the bit.

Also from Figs 6,10 and 14, the stress values predicted by HBRM showed a good agreement with that of the measured stress values. Hemphil et al 1993[12] emphasized that the Yield power law(HBRM) offer many advantages over the BPRM and PLRM because it more accurately characterizes mud behaviour across the entire shear rate range. The better accuracy of the HBRM can also be attributed to the fact that it accommodates the existence of a yield point (Bingham Plastic) as well as non-linearity of the shear stress to shear rate (Power law) [20].

The Casson rheological Model provides the best accuracy as shown in Figs.6,10 and 14 for all the three mud samples. This model provides the best information at both high and low shear rate conditions.

Measure of deviation of models from measured stresses

The following statistical methods were used to actually predict the degree of deviation of each model from the measured stresses.

1.Absolute Average Percentage Error ϵ_{AAP}

2.Standard Deviation of Average Percentage Error $SD\epsilon_{AAP}$

The E_{AAP} is given by the Equation (35)

$$\epsilon_{AAP} = \left[\frac{1}{N} \sum \left| \frac{(\tau_{measured} - \tau_{calculated})}{\tau_{measured}} \right| \right] * 100 \quad (35)$$

The standard deviation of average percentage error is obtained using Equation (36).

$$SD\epsilon_{AAP} = \sqrt{\frac{\sum f(\epsilon_{error} - \epsilon_{AAP})^2}{\sum f}} \quad (36)$$

Based on Equation (35), Table 7. shows the ϵ_{AAP} of the rheological models of the three mud samples.

Table 7: Absolute Average Percentage Error (ϵ_{AAP}) of the Rheological Models

| Mud Samples | PLRM | BPRM | HBRM | CRM |
|-----------------------------|----------|---------|---------|---------|
| RBDCO | 26.866 | 52.2811 | 11.1040 | 8.2819 |
| Trans-Esterified PKO | 19.09118 | 38.006 | 10.1125 | 9.51105 |
| Inter-Esterified PKO | 10.9053 | 35.8690 | 7.7478 | 6.9521 |

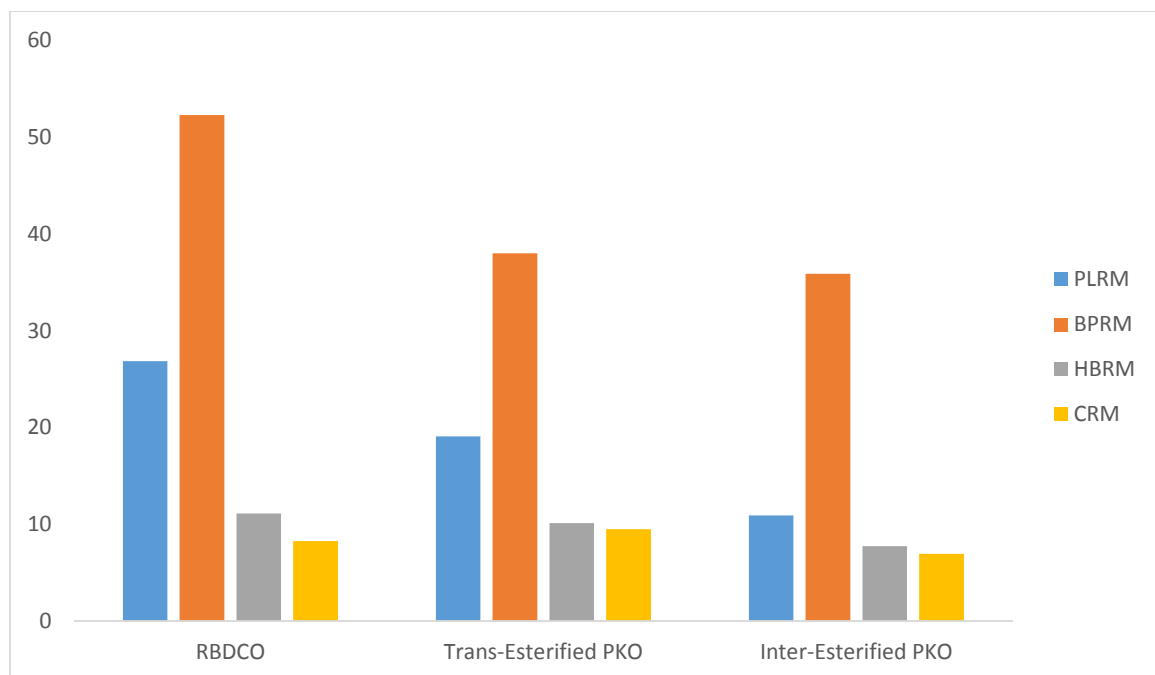


Figure 14: Absolute Average Percentage Error of Rheological Models.

From Table 7 and Figure 14, the highest absolute average percentage error (ϵ_{AAP}) was observed with BPRM for all the three mud samples while CRM showed the lowest absolute average percentage error. The HBRM also showed a promising accuracy with a lower absolute average percentage error.

Also from Equation (36), the standard deviation of average percentage error of the Rheological Models for the three mud samples is shown in Table 8.

Table 8: Standard Deviation of Average Percentage Error of the Rheological Models.

| Mud Samples | PLRM | BPRM | HBRM | CRM |
|-----------------------------|---------|---------|--------|--------|
| RBDCO | 16.7030 | 42.0458 | 7.0743 | 7.2658 |
| Trans-Esterified PKO | 14.1931 | 22.7016 | 6.8822 | 6.8480 |
| Inter-Esterified PKO | 7.5269 | 20.7437 | 5.1206 | 3.5643 |

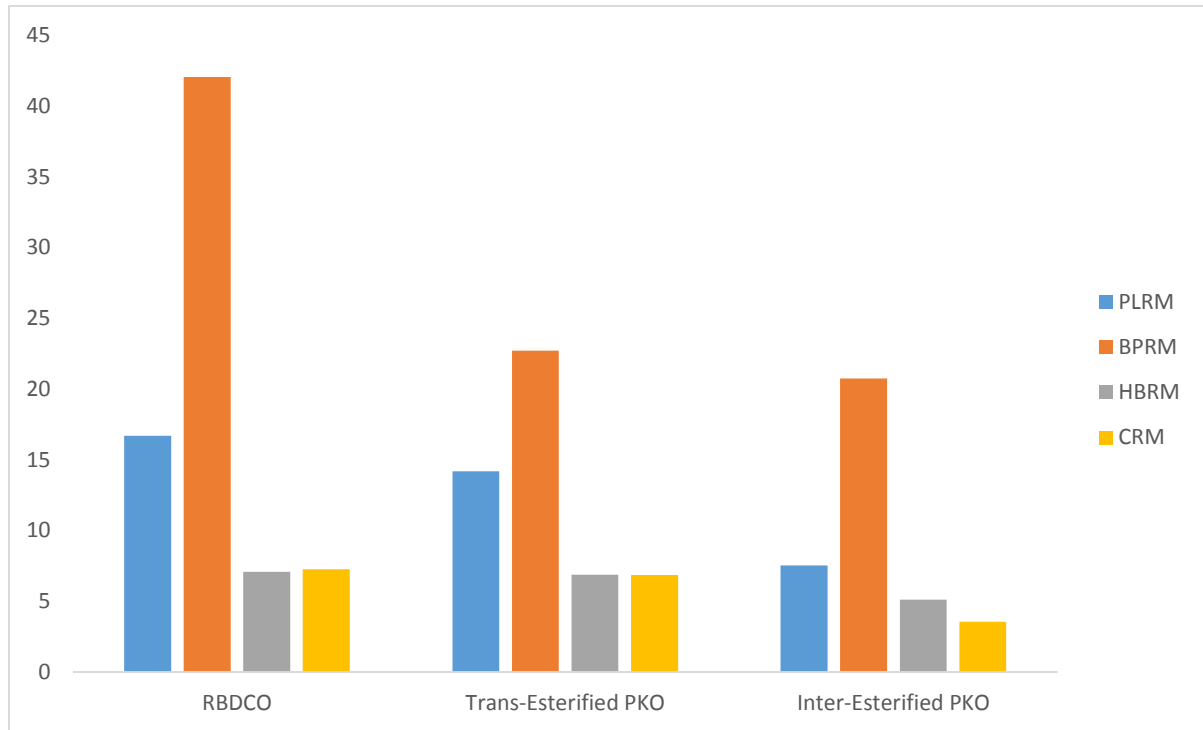


Figure 15: Standard Deviation of Average Percentage Error of Rheological Models.

Similarly, from Table 8 and Figure 15, the highest standard deviation of average percentage error ($SD\epsilon_{AAP}$) was seen in BPRM for all the three mud samples while the TRANSPKO and INTERPKO showed the least standard deviation of average percentage error with Casson rheological Model

CONCLUSIONS

An investigation has been made to accurately predict the best rheological model that can reliably characterize a synthetic based mud using empirical, theoretical and structural model and two statistical tools were employed to measure the degree of deviation of measured stresses from those predicted by the various models.

Some concluding observations from the investigation are.

- The Casson rheological model accurately characterizes mud behaviour across the entire low and

high shear rates conditions. This accuracy is attributed to the correction factor that is introduced to the yield stress and the plastic viscosity.

- The Hershel-Buckley rheological model also accurately predict mud behaviour across the entire low and high shear rates but higher accuracy is achieved with Casson Rheological Model.
- The Bingham plastic model does not predict accurately the behaviour of the drilling mud at very low shear rate as the case may be annulus and at very high shear rate as in the bit and hence, a yield stress and plastic viscosity correction factors are required.
- The power law rheological model gives better information at the onset of low shear rate condition but has a draw back at the start of high shear rate condition.

ACKNOWLEDGEMENT

The authors are very grateful to the Chancellor of Covenant University and the university management team for their unalloyed support for research and development without which this research work would not have seen the light of the day.

REFERENCES

- [1] Dardir, M.M., Ibrahime, S, Soliman, M., Deasouky, S.D., and Hafiz. A.A., 2014, "Preparation of some estramides as Synthetic Based Drilling Fluid," *Egyptian Journal of petroleum*. 23(1), pp. 35-43.
- [2] Burke, C.J., and Veil, J.A., 1995, "Synthetic-Based Drilling Fluids have many environmental pluses". *Oil and Gas Journal*, 93, pp. 59-64.
- [3] Thivolle, S. ,2004, "Rheological Behaviour of Drilling Muds, characterization using MRI Visualization". *Journal of Oil and Gas Science and Technology*, 59(1), pp 23-29.
- [4] Krieger, I.M.; and Dougherty, I.J. ,1959, "A mechanism for Non-Newtonian Flow in Suspension of Rigid Spheres". *Journal of Rheology* 3, pp.137-152.
- [5] Coussot, P., Ngugen,O.D.,Huynh,H.T.,and Bonn,D. ,2002, "Viscosity bifurcation in Thixotropic, Yielding Fluids". *Journal of Rheology*,46, pp. 573-589.
- [6] Bird, R.B.; Grance, D.and Yarusso, B.J. ,1982, "The Rheological and flow of Viscoplastic Materials". *Review in Chemical Engineering* (1), pp .1-70
- [7] Reiner, M. 1926." Kolloid Z." 39, pp. 80-87
- [8] Casson, M. ,1959, "The Rheology of Disperse Systems". Pergamon press, London.
- [9] Herschel, W.H.; and Buckley, R.,1926. "Konsistenzmessungen von Gummi Benzollösungen." *Kolloid Z* 39; pp.291-300.
- [10] Bingham, E.C. ,1922, "Fluidity and plasticity". MC Graw-hill, New York.
- [11] Hemphill, T.; Campos, W.; and Pilehvari, A.,1993, "Yield Power Law Model more accurately predicts Mud Rheology". *Oil and Gas Journal*,91, pp .34
- [12] Barnes, H.A., and Walters, K.,1985, "The yield stress Myth". *Rheological Acta*, 24, pp.323-326
- [13] Kalili-Garakani, A.; Mehrnia, M.R.; Mostofi, N.,and Sarrafzadeh, M.H.,2011,"Analyses and Control Fouling in an Airlift Membrane Bioreactor.CFD Simulation and Experimental studies," *Process Biochem*; 46(5); pp.1138-1145.
- [14] Steffe, J.F.,1996," *Rheological Methods in Food Process Engineering*" (6thed) Freeman press. East Lansing USA.ISBN 0-9632036-1-4.
- [15] Fann Instrument Company (2013). Model 35 Viscometer Instruction Manual, Fann Instrument Company, Houston, Texas, pp. 44.
- [16] Lauzon, R.V.; and Reid, K.I. (1979)." New Rheological Model Offers Field Alternative." *Oil and Gas Journal* 51.
- [17] Becker, R.G.; Morgan, W.C.; Chin, J.E.; and Griffith, J.,2003, "Improved Rheology Model and Hydraulics Analysis for Tomorrow's Wellbore Fluids Application." *Society of Petroleum Engineers*, Tulsa,Oklahoma.
- [18] Barnes, H.A.,1997," Thixotropic –a review." *Journal of Non-Newtonian Fluid Mechanics*, 70, pp.1-33
- [19] Power, D., and Zamora, M.,2003, "Drilling Fluid Yield Stress-Measurement Techniques for Improved Understanding of Critical Drilling Fluid Parameters". *AADE Technical Conference*, Houston.

APPENDIX A

Mud Samples Composition

| MUD COMPONENT | VOLUME (ml) or MASS (g) |
|--------------------------|-------------------------|
| Base Oil | 260ml |
| Primary Emulsifier | 8ml |
| Secondary Emulsifier | 4ml |
| Wetting Agent | 2ml |
| Viscosifiers | 4grams |
| Fluid Loss Additive | 7grams |
| Calcium Chloride | 18grams |
| Water (H ₂ O) | 72ml |
| Weighting Agent | 75 grams |